ANNUAL REVIEWS

Annual Review of Biophysics

Molecular Level Super-Resolution Fluorescence Imaging

Niels Radmacher,[1] Alexey I. Chizhik,[1] Oleksii Nevskyi,[1] José Ignacio Gallea,[1] Ingo Gregor,[1] and Jörg Enderlein[1,2]

[1]Third Institute of Physics – Biophysics, Georg-August-University, Göttingen, Germany; email: jenderl@gwdg.de

[2]Cluster of Excellence "Multiscale Bioimaging: from Molecular Machines to Networks of Excitable Cells" (MBExC), Universitätsmedizin Göttingen, Göttingen, Germany

Annu. Rev. Biophys. 2025. 54:163–84

The *Annual Review of Biophysics* is online at biophys.annualreviews.org

https://doi.org/10.1146/annurev-biophys-071524-105321

Keywords

single-molecule localization microscopy, expansion microscopy, fluorescence lifetime super-resolution microscopy, molecular resolution

Abstract

Over the last 30 years, fluorescence microscopy, renowned for its sensitivity and specificity, has undergone a revolution in resolving ever-smaller details. This advancement began with stimulated emission depletion (STED) microscopy and progressed with techniques such as photoactivatable localization microscopy and stochastic optical reconstruction microscopy (STORM). Single-molecule localization microscopy (SMLM), which encompasses methods like direct STORM, has significantly enhanced image resolution. Even though its speed is slower than that of STED, SMLM achieves higher resolution by overcoming photobleaching limitations, particularly through DNA point accumulation for imaging in nanoscale topography (DNA-PAINT), which continuously renews fluorescent labels. Additionally, cryo-fluorescence microscopy and advanced techniques like minimal photon fluxes imaging (MINFLUX) have pushed the boundaries toward molecular resolution SMLM. This review discusses the latest developments in SMLM, highlighting methods like resolution enhancement by sequential imaging (RESI) and PAINT-MINFLUX and exploring axial localization techniques such as supercritical angle fluorescence and

metal-induced energy transfer. These advancements promise to revolutionize fluorescence microscopy, providing resolution comparable to that of electron microscopy.

Contents

1. INTRODUCTION

Fluorescence microscopy is one of the most powerful research tools in the life sciences due to its extreme sensitivity (down to single molecules) and specificity (ability to specifically label targets of interest by specific fluorescent dyes). In the last 30 years, fluorescence microscopy has seen a tremendous revolution concerning its capability to resolve smaller and smaller details. This started with the development of stimulated emission depletion (STED) microscopy by Hell & Wichmann (38) and was continued with the quasi-simultaneous development of photoactivatable localization microscopy (PALM) by Betzig et al. (4), fluorescent PALM (fPALM) by Hess et al. (41), and stochastic optical reconstruction microscopy (STORM) by Zhuang and colleagues (81). Both PALM and STORM are based on the localization of single molecules with a localization precision that is tremendously better than the width of a single-molecule image itself (which is basically the width of the point spread function of the microscope used). Nowadays, all methods based on the localization of single emitters are subsumed under the name single-molecule localization microscopy (SMLM). With direct STORM (dSTORM), Sauer and colleagues (35) demonstrated how to use almost any fluorescent dye for realizing STORM, and this method became extremely popular and widely applied. Compared with STED microscopy, SMLM is technically much simpler to realize because it requires only a conventional wide-field microscope with a sufficiently sensitive wide-field camera, and it can routinely achieve a much-higher-resolved final image. The disadvantage of SMLM is that it is intrinsically slow, because it requires the recording of thousands of individual images for one final super-resolved image (although exceptions apply, see, e.g., References 90 and 101). Thus, when it comes to image speed or live-cell imaging, STED certainly performs better than SMLM does.

The final resolution of an SMLM image is determined solely by the number of photons that can be detected from a single fluorescent molecule until its photobleaching (or switching into a dark state). Although many different techniques to extend the survival time of fluorescent dyes until bleaching have been developed (among them cryo-fluorescence microscopy, which is discussed in Section 6), there is on average a limit of approximately 10^3 to 10^4 photons until photobleaching for most dyes at room temperature and in an aqueous environment. Thus, when also taking into account other effects that impact the final resolution, such as camera pixel size, scattering or autofluorescent background, and electronic noise (for a quantitative analysis, see Reference 66), the typical achievable resolution of SMLM is approximately 20 nm.

This limitation due to photobleaching has fundamentally changed only with the advent of point accumulation for imaging in nanoscale topography (PAINT) microscopy, which was first developed by Sharonov & Hochstrasser (92). In PAINT, switching of fluorescent labels is achieved not by an actual photophysical switching between a nonfluorescent dark off-state and a fluorescent on-state but by reversible binding of a fluorescent label (imager) to a target of interest. PAINT has become the most popular method in the SMLM community with the introduction of its modification, DNA-PAINT (50), which uses the versatility of DNA hybridization for realizing such reversible binding between imager and target. DNA-PAINT completely lifts the restrictions usually imposed on SMLM by photobleaching. Because the label at a given target is constantly exchanged, PAINT allows for, in principle, infinite localization precision (and thus image resolution), provided that one is able to associate repeated binding and unbinding events to one and the same target.

Another way of circumventing the restrictions of photobleaching is cryo-fluorescence microscopy. When cooling a sample to liquid nitrogen or liquid helium temperatures, rotational and vibrational degrees of freedom of molecular motion are frozen out, which dramatically improves the photostability of fluorescent molecules. This enhanced photostability promises to allow for nanometer localization precision in SMLM, but it also mostly suppresses any photoswitching/intensity blinking, which is one of the prerequisites of SMLM.

One of the latest additions to the zoo of SMLM methods is minimal photon fluxes imaging (MINFLUX) (3), which pushes the accuracy of single-molecule localization per a given photon budget to its limit by using a clever excitation and detection scheme. MINFLUX demonstrated subnanometer localization of single molecules with unprecedented low photon detection numbers and has thus become the strongest contender against DNA-PAINT for molecular resolution SMLM.

In this review, we report on the latest developments in fluorescent SMLM for molecular resolution microscopy. The last few years have seen an extreme push in SMLM resolution, which now comes close to the resolution typically achieved with electron microscopy. Excellent reviews of extreme-resolution fluorescence microscopy have been previously published (2, 59); however, the field is evolving quickly and we think it deserves a timely update, which is the main goal of this review.

2. ÅNGSTRÖM-RESOLUTION DNA-PAINT

As mentioned in Section 1, DNA-PAINT is one of the most versatile SMLM techniques (**Figure 1*a***), promising true molecular resolution with moderate technical complexity. In DNA-PAINT, specific sites on a target are labeled with short single strands of DNA that can reversibly hybridize with fluorescently labeled conjugate DNA strands (imager strands) added to the sample solution. This reversible binding of imager strands leads to continuous renewal of fluorescent dyes at the target site, thus overcoming the photodestruction barrier of conventional PALM/dSTORM

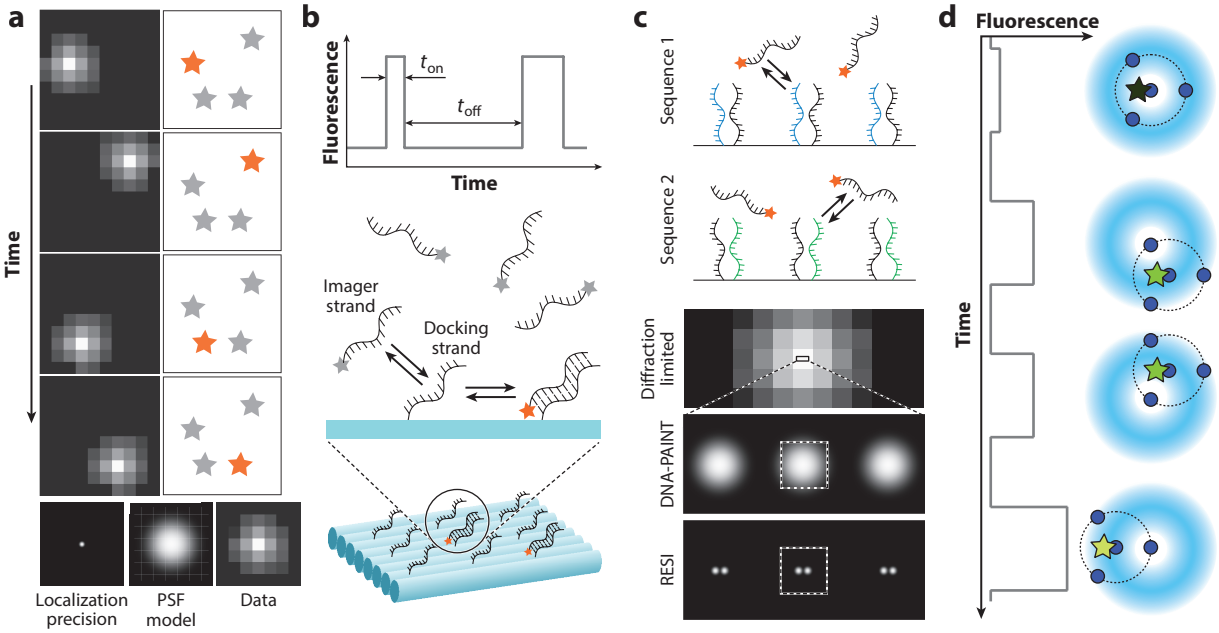

Figure 1

Principle of single-molecule localization microscopy techniques. (*a*) STORM achieves high resolution by utilizing the stochastic activation and precise localization of individual fluorescent molecules. STORM relies on photoswitchable fluorophores, which can be toggled between fluorescent and dark states. Only a sparse subset of these fluorophores is activated at any given time, ensuring that their emission profiles do not overlap. Each activated fluorophore emits light that is captured as a diffraction-limited spot. The center of this spot is calculated with high precision to determine the fluorophore's exact position. This process is repeated many times, with different subsets of fluorophores being activated and localized in each cycle. The accumulation of these precise localizations over many cycles allows for the reconstruction of a super-resolved image, where individual molecules are positioned with nanometer accuracy. (*b*) DNA-PAINT is a super-resolution microscopy technique that utilizes transient binding between short, single-stranded DNA imager strands and their complementary docking strands attached to target molecules. This technique achieves high spatial resolution by accumulating imaging data over time, where each binding event produces a fluorescence signal at a precise location. The repeated binding and unbinding of imager strands result in the stochastic appearance of fluorescence points, which are then localized with nanometer precision. By accumulating many such points, one can reconstruct a high-resolution image of the target structure. (*c*) RESI is a variant of DNA-PAINT where closely localized targets are sequentially labeled using different imager strand and target strand combinations. This approach allows for the collection of photons from each target over numerous binding–unbinding cycles, enabling the precise localization of targets with Ångström-level resolution. (*d*) MINFLUX is a super-resolution microscopy technique that achieves ultrahigh resolution by combining fluorescence imaging with a targeted illumination approach using a structured illumination with a zero-intensity point (usually doughnut-shaped intensity distribution). Unlike traditional methods that rely on high photon counts, MINFLUX precisely determines the position of fluorescent molecules by triangulating them. This is achieved by directing a doughnut-shaped laser beam at the target, and the position is calculated on the basis of the proximity of the molecule to the dark center of the beam. MINFLUX can achieve resolutions as low as 1–3 nm, making it one of the most precise imaging techniques available. Abbreviations: DNA-PAINT, DNA point accumulation for imaging in nanoscale topography; MINFLUX, minimal photon fluxes imaging; NA, numerical aperture; PSF, point spread function; RESI, resolution enhancement by sequential imaging; STORM, stochastic optical reconstruction microscopy.

(**Figure 1*b***). This barrier limits the maximum number of detectable fluorescence photons per target site and, consequently, the maximum achievable accuracy of localizing a single molecule.

In a recent paper, Sauer and colleagues (39) demonstrated that all fluorescent molecules begin to photophysically interact if their distance is less than approximately 10 nm. Due to this interaction, two separate dye molecules start to appear as one molecule when they are less than 10 nm apart, making it impossible to resolve structural details below this threshold with PALM

or STORM, where dyes are covalently attached to target sites. This photophysical interaction is not a principal problem for PAINT: By choosing the right imager strand concentrations and binding kinetics, one can minimize the probability that two simultaneously bound dyes will be closer than 10 nm.

Moreover, by selecting orthogonal binding sequences for closely separated target sites, one can sequentially image and localize each site with virtually unlimited localization accuracy (by collecting signals for each site over many binding and unbinding events). This approach results in true Ångström-scale molecular resolution, as demonstrated by Jungmann and colleagues in their seminal paper (78), where they named this approach resolution enhancement by sequential imaging (RESI) (**Figure 1*c***). This groundbreaking paper presents a relatively straightforward and potentially widely applicable method for achieving molecular resolution SMLM, potentially revolutionizing fluorescence imaging of molecular structures with a resolution that competes with electron microscopy.

3. MINFLUX

The biggest competitor in SMLM for achieving molecular resolution is MINFLUX (3). The core idea of MINFLUX is to scan a sample with structured excitation that features a zero-intensity singularity, typically a doughnut-shaped) beam excitation profile (**Figure 1*d***). The scan path is chosen to maximize the information about the emitter's location. The method leverages the principle that when the emitter's position is close to the singularity, even small shifts of the excitation relative to the emitter's position result in significant relative changes in observable intensity.

Since the first publication on MINFLUX (3), the technique has seen several advancements, particularly in 3D and multicolor imaging (33), demonstrating its ability to image protein arrangements in three dimensions (e.g., in individual mitochondria) with nanometer resolution (72). One unique feature of 3D-MINFLUX is its ability to achieve nearly isotropic nanometer resolution by generating a suitable 3D excitation intensity distribution with a zero-intensity singularity in the center. This capability is difficult to achieve with conventional wide-field SMLM, where the axial and lateral resolutions typically differ by a factor of 2 to 3 due to the different transmission efficiencies of axial and transverse spatial frequencies by a wide-field microscope.

The most significant hallmark of MINFLUX is its unparalleled localization accuracy per photon, which can be one order of magnitude better than what is achievable with wide-field SMLM. This makes MINFLUX the method of choice for fast and high-precision single-molecule tracking, with temporal resolution down to microseconds (86), and for tracking individual GFP-tagged proteins in bacteria (9). Using MINFLUX's unmatched tracking capabilities, Hell and colleagues (115) recently discovered a new locomotion mode of the motor protein kinesin-1 that had never been observed before.

The original implementation of MINFLUX by Balzarotti et al. (3) was technically complex. However, several groups have significantly improved the technique, making it more accessible. The first improvement replaced the complex scanning of the doughnut beam with electro-optical deflectors with an excitation scheme involving three independently and spatially shifted doughnut beams that are sequentially switched on and off in time [pulsed interleaved MINFLUX (p-MINFLUX)] (61). This approach is technically simpler than the electro-optical deflection of a single beam. The next major advancement was by Stefani and colleagues (120), who introduced raster scan MINFLUX (RASTMIN). Their work showed, both theoretically and experimentally, that one can achieve localization performance similar to that of the original MINFLUX by using a regular raster scan of a doughnut beam instead of the complex scan sequence of the original method. This simplification greatly enhances the technique's accessibility. Finally, Deguchi & Ries (21) recently simplified 3D-MINFLUX by using a variable phase plate.

When comparing MINFLUX to DNA-PAINT-RESI, several aspects stand out. The primary difference is that MINFLUX is inherently a sequential method, while DNA-PAINT is highly parallelized. MINFLUX localizes single molecules sequentially and requires a specific scan trajectory for each localization, making the method slow (approximately one localization per second), which can lead to total imaging times on the order of hours for small organelles such as single mitochondria. In contrast, DNA-PAINT can be much faster because it is based on wide-field imaging, allowing for simultaneous localization of hundreds of molecules. However, MINFLUX tends to have better 3D resolution capabilities, although DNA-PAINT-RESI compensates for this by collecting more photons (observing more binding and unbinding events). Technically, MINFLUX remains more complex than DNA-PAINT, which requires only a sufficiently sensitive and mechanically stable wide-field microscope, despite the advancements of p-MINFLUX and RASTMIN. The greatest advantage of MINFLUX over DNA-PAINT is its ability to rapidly track single molecules with nanometer spatial and microsecond temporal resolutions. However, as shown by Ostersehlt et al. (70), combining DNA-PAINT with MINFLUX can overcome the photostability barrier of conventional covalent labeling of a target, ultimately enhancing the achievable resolution of MINFLUX.

4. ADVANCED SINGLE-MOLECULE LOCALIZATION TECHNIQUES

When it comes to molecular resolution, any advancement for better localization accuracy or elimination of optical aberrations becomes important. In this section, we consider several new methods that improve localization and circumvent aberrations.

4.1. Patterned Illumination

As first demonstrated by Gustafsson (31), the use of structured illumination in wide-field microscopy can improve spatial resolution by up to a factor of 2 (**Figure 2*a***). This is the principle of structured illumination microscopy (SIM), now a common technique in wide-field fluorescence microscopy. In SIM, the sample is illuminated sequentially with structured illumination at various lateral positions and different orientations of the illumination pattern (typically a 1D sinusoidal excitation grating). From the recorded images at different pattern positions and orientations a doubly resolved final image can be computed (36).

Recent publications have transferred the core idea of SIM, namely using structured illumination for resolution doubling, to the realm of SMLM. The first of these was by Reymond et al. (80), in which the authors demonstrated a doubling of the localization accuracy of SMLM using structured illumination. They generated the sinusoidally modulated intensity pattern using a digital mirror device and named their method structured illumination-based point localization estimator with enhanced precision (SIMPLE). Reymond et al. (79) presented a particularly interesting realization of this concept; they measured the modulated fluorescence intensities of single emitters in a precisely shifted structured illumination pattern to achieve enhanced localization accuracy in three dimensions.

Shortly after SIMPLE was published, Cnossen et al. (18) realized the same idea by switching between different sinusoidal excitation patterns using fast Pockels cells, naming their method SIMFLUX, in allusion to the zero-intensity singularities in the excitation intensity distribution characteristic of MINFLUX. In a subsequent paper, these authors extended the idea to 3D SMLM (107).

The name SIMFLUX is somewhat misleading: MINFLUX relies on a peculiar scan pattern of the doughnut excitation beam tailored to the constantly updated position estimate of a molecule to be localized, whereas SIMFLUX cannot update and adapt the relative pattern position to the

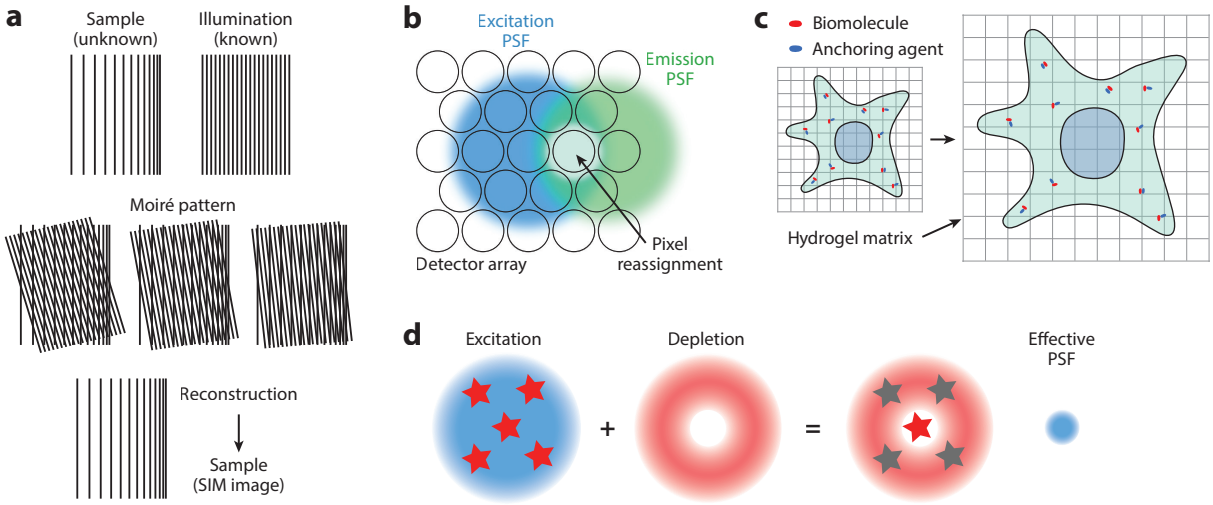

Figure 2

Techniques that can be used for increasing resolution in single-molecule localization microscopy. (*a*) SIM is a super-resolution imaging technique that enhances the resolution of fluorescence microscopy by using patterned light to illuminate the sample. The interference of this structured light with the sample's fluorescence produces moiré patterns that contain high-frequency spatial information. By capturing multiple images with different illumination patterns and then computationally reconstructing them, SIM can achieve a resolution approximately twice that of conventional light microscopy, down to approximately 100 nm. SIM is particularly useful for live-cell imaging due to its relatively low phototoxicity and fast acquisition times. (*b*) ISM is a super-resolution imaging technique that enhances the resolution of confocal microscopy. In ISM, a confocal microscope is equipped with an array detector (e.g., a camera) instead of a single-point detector. The size of the array pixels is small enough so that each scan image recorded by one pixel has a nearly doubled resolution compared to that of a conventional confocal microscope with a large confocal aperture. However, despite the small pixel size, no light is lost due to the presence of many pixels in the array detector. ISM effectively doubles the resolution compared to conventional confocal microscopy, achieving lateral resolutions of approximately 120 nm and providing sharper, more detailed images. (*c*) ExM is a super-resolution technique that physically enlarges biological samples by embedding them in a swellable hydrogel. The sample is chemically anchored to the hydrogel, which is then expanded isotropically, allowing standard microscopes to visualize nanoscale structures with enhanced resolution. ExM can achieve effective resolutions of approximately 60 to 70 nm or even better when combined with other super-resolution methods. It is widely used for detailed imaging of cellular structures, proteins, and nucleic acids in various biological contexts. (*d*) STED microscopy is a super-resolution imaging technique that improves optical resolution by selectively deactivating fluorophores. In STED, a focused laser excites fluorophores, while a second, doughnut-shaped laser beam depletes the excited state of fluorophores at the periphery, leaving only a small central region to emit light. This process effectively sharpens the PSF, allowing the microscope to achieve resolutions well below the diffraction limit, down to 20–30 nm, making it ideal for detailed imaging of subcellular structures. STED microscopy can be, to some extent, considered a technical precursor to MINFLUX (doughnut-shaped excitation, sequential scanning). Abbreviations: ExM, expansion microscopy; ISM, image scanning microscopy; MINFLUX, minimal photon fluxes imaging; PSF, point spread function; SIM, structured illumination microscopy; STED, stimulated emission depletion.

estimated localization of single molecules. As a result, SIMFLUX offers only a two-fold improvement in localization accuracy (similar to SIMPLE), whereas MINFLUX improves localization accuracy by more than one order of magnitude for the same photon budget.

A drawback of combining SIM and SMLM is that a molecule must remain in the fluorescent on-state for the entire sequence of SIM excitation patterns. This is not an issue for an alternative method that combines structured illumination and SMLM: image scanning SMLM (iSMLM). The principle of image scanning microscopy (ISM) was first proposed by Sheppard (94) in a theoretical paper in 1988 and is based on the same physical principles as those of SIM. In ISM, the diffraction-limited excitation focus of a conventional confocal laser scanning microscope (CLSM) is used as the structured illumination, and at each scan position, a small image of the illuminated

region is recorded (in contrast, a conventional CLSM records only the total fluorescence signal generated at a given scan position). Using a dedicated algorithm, ISM generates a doubly resolved final image from the stack of recorded mini-images (67). This concept can also be used to double the localization accuracy of SMLM. This idea was experimentally realized as iSMLM by Radmacher and colleagues (75). In their paper, the authors nearly doubled the localization accuracy, achieving a lateral resolution of approximately 5 nm for a photon budget of approximately 1,500 photons per molecule localization. In a recent theoretical study, the authors claim that by applying a sophisticated data analysis, iSMLM can go beyond even a doubling of resolution, although experimental confirmation is yet to be done. Finally, a theoretical study by Slenders & Vicidomini (98) discusses the application of ISM to also improve MINFLUX localization accuracy, and they named this method ISM-FLUX. Their group (7) has applied this idea to the fast 3D tracking of single molecules.

The advantage of iSMLM over SIM-SMLM is that it requires only equipping a conventional CLSM with a sufficiently sensitive and fast detector array (**Figure 2*b***) instead of generating complex excitation patterns as in SIM. Recent advances in single photon avalanche diode (SPAD) array fabrication (8, 10, 54, 97) have made such detectors widely commercially available, which will certainly spur their application for ISM and iSMLM. Moreover, these detectors offer the option of fluorescence lifetime imaging microscopy (FLIM), as discussed in Section 4.2. Finally, iSMLM is more relaxed than SIM-SMLM concerning the survival or on-state duration of a fluorescent molecule during image acquisition. Additionally, iSMLM shows an improved signal-to-background ratio compared to wide-field-based SIM-SMLM due to its intrinsic confocality inherited from being based on a CLSM.

4.2. Fluorescence Lifetime

The core goal of molecular scale SMLM is to record the relative positions of different labels within the same molecule or small molecular complexes. As already discussed in Section 2, this is achieved in RESI (78) by sequentially imaging different target sites using orthogonal DNA hybridization sequences. However, this method is inherently slow, as it requires a full DNA-PAINT localization cycle for each target site. In conventional SMLM, multicolor labeling is often used to image several targets simultaneously. Yet, on a molecular scale, chromatic aberrations that are never completely absent in real-world optical systems can easily introduce localization errors of dozens of nanometers.

An attractive alternative to multicolor imaging is FLIM, where different targets are labeled with dyes that have similar excitation and emission spectra but different fluorescence lifetimes. Historically, the core obstacle to applying this concept to SMLM was the lack of suitable wide-field-camera systems capable of picosecond/nanosecond fluorescence lifetime measurements and sensitive enough for single-molecule detection and localization. This has changed recently with two new approaches. Oleksiievets et al. (69) used a novel commercially available wide-field FLIM camera, the LINCam (Photonscore, Magdeburg, Germany), to implement fluorescence lifetime SMLM (FL-SMLM) and demonstrate its multiplexing capability for simultaneous SMLM of several targets. Although the camera has a quantum yield of detection of only approximately 15% in the blue spectral region and as low as 5% in the red spectral region, it boasts close-to-zero electronic noise, allowing for high signal-to-noise measurements despite the low quantum yield. The primary downside of this system is its high price, which limits its wider application.

An interesting alternative to this commercial wide-field FLIM camera was proposed by Bowman et al. (6). The authors used clever nanosecond-fast switching of the optical detection path between different areas of a conventional camera by way of a custom fast-switching Pockels

cell. By applying pulsed (picosecond pulses) wide-field excitation and switching the optical detection path a few hundred picoseconds/few nanoseconds after each excitation, they generated two images capturing the fluorescence light in two different nanosecond time windows after excitation. From this information, Bowman et al. deduced the mean fluorescence decay time of imaged single molecules.

Another approach is to use a CLSM, which was not previously used for SMLM due to its slower image acquisition rate (each image requires sequential scanning of the field of view) and low duty cycle (the excitation focus remains only a small fraction of the total image time over the position of a single molecule). However, for FL-SMLM, a CLSM with pulsed excitation, equipped with single-photon-sensitive point detectors (usually SPADs) and accompanied by time-correlated single-photon data analysis, becomes an interesting option. The first realization of FL-SMLM with a CLSM was achieved by the groups of Enderlein and Sauer (103), using the fluorescence lifetime capability for multiplexing (i.e., simultaneous imaging of different targets in the same spectral window). A subsequent study compared the wide-field LINCam-based FL-SMLM and the CLSM-based FL-SMLM. The surprising result was that although the CLSM-based system has an overall lower detection efficiency than the LINCam-based system does, the latter performs comparatively well (in terms of achievable localization accuracy per detected photon budget) in the blue spectral region and becomes inefficient only for fluorophores in the red spectral region (68). Finally, an in-depth study by Thiele et al. (105) investigated optimal algorithms for extracting the fluorescence lifetime of single molecules in FL-SMLM data and found that simple tail-fitting of fluorescence decay curves performs only slightly worse than much more complex data evaluation procedures based on full deconvolution and Bayes probabilistic analysis. This finding is important for applications of FL-SMLM in molecular scale super-resolution microscopy, especially in the context of axial localization via fluorescence lifetime modulation by metal-induced energy transfer (MIET) (see Section 5).

4.3. Expansion Microscopy

Nearly all the methods and approaches to molecular level super-resolution fluorescence microscopy discussed here are based on SMLM. The notable exception, which is an interesting alternative, is expansion microscopy (ExM) (13, 27). In ExM, a sample is embedded in a swellable polymer, which is then isotropically expanded, effectively increasing the distance between individual molecules (**Figure 2*c***). ExM involves several key steps. In the anchoring step, the sample is treated with a cross-linking agent that attaches target molecules to a polymerizable gel. In the polymerization step, a hydrogel is formed around the sample through radical polymerization, integrating the anchored molecules. In the homogenization step, the sample is treated to remove noncovalent interactions, enabling uniform expansion. And finally, in the expansion step, the hydrogel is immersed in water, which causes it to swell isotropically, increasing the physical size of the sample. Typically expanding the sample by a factor of 4 to 5 allows conventional optical microscopes to achieve nanoscale resolution. The key advantage of ExM is its ability to use standard fluorescent dyes and microscopes, making it accessible and straightforward for a wide range of applications in biological research.

A core issue of ExM is the fluorescent labeling of the sample. This can be performed either before or after the expansion process, depending on the specific requirements of the experiment (17, 106). Preexpansion labeling involves labeling the sample with fluorescent markers before embedding it in the hydrogel and expanding it. This method is straightforward but may result in a lower effective label density after expansion, as the distance between fluorophores increases proportionally with the expansion factor. Preexpansion labeling is particularly useful when

targeting proteins, nucleic acids, or other biomolecules with specific antibodies, dyes, or probes that are introduced before the expansion process. Alternatively, in postexpansion labeling, the sample is first expanded and then labeled. This method allows for higher effective label densities, as the fluorophores can be introduced into the expanded structure, filling the increased volume. Postexpansion labeling can also reveal epitopes that were previously inaccessible due to molecular crowding or steric hindrance in the native, unexpanded state. This technique is particularly essential when resolving structural details at the molecular level.

Achieving high label densities is crucial for maximizing the resolution benefits of ExM. Several approaches achieve high label densities in ExM (13, 111). Using high concentrations of antibodies or fluorescent probes during the labeling process ensures that more binding sites are occupied. Using smaller probes such as small-molecule fluorescent dyes or nanobodies instead of bulky antibodies enables better labeling efficiency and better access of the labels to the targets. And, as mentioned above, postexpansion labeling allows for the use of smaller molecules that can penetrate the expanded hydrogel matrix more effectively, resulting in denser and more uniform labeling. Finally, multiple rounds of labeling can be used to increase the overall label density, especially in dense or complex structures.

In a recent paper, Sauer and colleagues (123) combined ExM with SMLM to push the resolution to true molecular levels. Collaborating with the groups of Rizzoli and Boyden, they (91) demonstrated that it is possible to resolve the structure of single antibody molecules using ExM together with super-resolution optical fluctuation microscopy, which they termed one-step nanoscale expansion (ONE) microscopy. Additionally, using a combination of expansion and SMLM, Chang et al. (12) resolved the ultrastructural composition of distal appendages in expanded mammalian centrioles with nanometer resolution, an impressive achievement in a cellular context.

The challenge of expansion SMLM, compared to SMLM of nonexpanded samples, is to ensure the reproducibility and fidelity of the expansion process while avoiding artifacts introduced by the expansion protocol and the chemicals used for digestion and swelling of the sample. For example, the position of organic fluorescent labels may change due to the breaking of the covalent bond between the label and target during sample preparation, or the final labeling efficiency may be much lower than in conventional SMLM, leading to very sparse localizations. Nonetheless, ExM combined with super-resolution imaging (such as ONE microscopy) is a promising avenue for molecular level super-resolution, and we are only beginning to see its potential.

5. AXIAL SINGLE-MOLECULE LOCALIZATION

A major challenge of super-resolution microscopy is precisely localizing molecules not only laterally but also axially to achieve true 3D super-resolution. Conventional SMLM employs various methods for axial localization, with the most popular being astigmatic imaging (43), biplane imaging (49), and point spread function engineering (55, 73, 93, 108). However, these methods typically yield axial resolutions that are two to three times poorer than their lateral counterparts, due to the limited transfer of axial spatial frequencies compared to lateral ones through a microscope objective (24).

This ratio of transmitted frequencies is reversed in interferometric methods, where a sample is observed from both sides with two objectives. The concept of imaging a sample from both sides with high-numerical-aperture objectives to enhance the axial resolution of a CLSM was pioneered by Hell & Stelzer (37) in 1992 and is known as 4Pi microscopy (alluding to the nearly full solid angle of 4π over which fluorescence is collected) (22) (**Figure 3*c***). The core idea is to interfere two counterpropagating coherent and focused laser beams in the focal region, generating

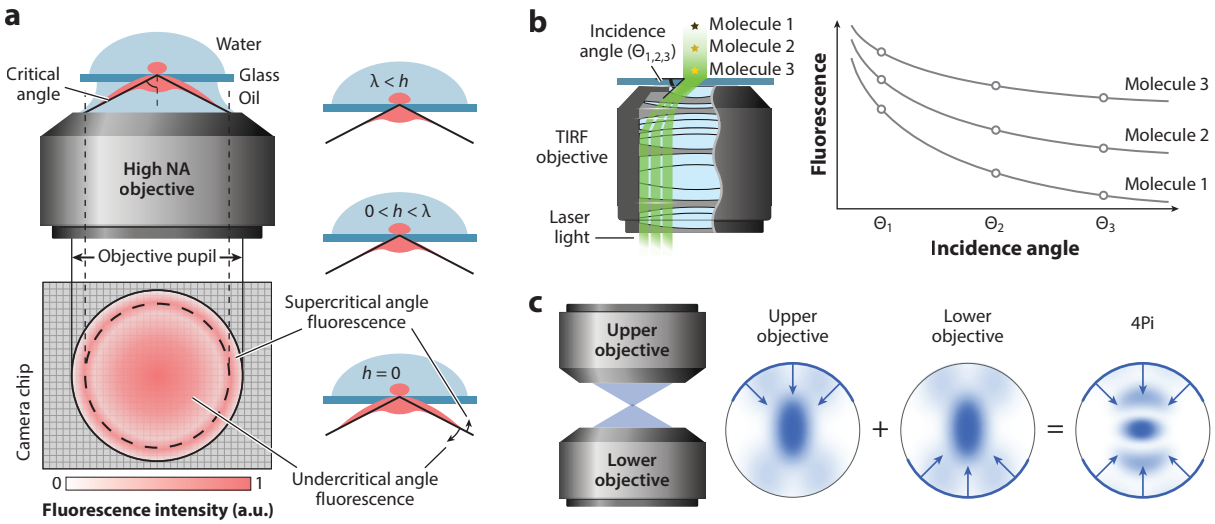

Figure 3

Principle of axial resolution enhancement techniques and cryo-microscopy. (*a*) SAF imaging is a microscopy technique that enables extreme axial resolution near a glass–water interface. It leverages the fact that the near field of fluorescent emitters in water can couple to far-field propagating modes above the critical angle of total internal reflection in the glass, a process that is extremely sensitive to the distance of a fluorophore from the interface. By collecting these SAF signals, SAF imaging allows for axially localizing fluorescent structures with nanometer resolution. This is particularly interesting for studying membrane-associated processes and structures close to the cell surface. (*b*) VA-TIRF microscopy is an advanced imaging technique that allows precise control over the penetration depth of the evanescent wave used to excite fluorophores near the sample surface. By varying the angle of the incident laser light, VA-TIRF can selectively illuminate and image structures at different depths, typically within 100–200 nm of the surface, and then localize them with nanometer accuracy. This technique is particularly useful for studying dynamic processes at the cell membrane and provides high-contrast images with reduced background fluorescence. (*c*) 4Pi imaging is a super-resolution microscopy technique that significantly improves axial resolution by using two opposing objective lenses to collect light from both sides of a sample. This setup creates an interference pattern between the light waves, which enhances the resolution along the optical axis, achieving up to a sevenfold improvement compared to conventional microscopy. 4Pi microscopy is particularly useful for imaging thick biological samples (beyond the range that can be seen by SAF or VA-TIRF) and capturing detailed 3D structures, making it ideal for studying complex cellular components and large macromolecular assemblies. Abbreviations: NA, numerical aperture; SAF, supercritical angle fluorescence; VA-TIRF, variable-angle total internal reflection fluorescence.

a standing intensity modulation along the optical axis with a modulation periodicity of one-quarter of the wavelength. Scanning this modulated excitation intensity distribution over a sample in three dimensions yields a 3D image with enhanced axial resolution, while the lateral resolution remains that of a conventional CLSM. Additionally, interfering the fluorescence emission collected by the two objectives can further double the axial resolution (32).

With the advent of super-resolution microscopy, the core idea of 4Pi microscopy was applied to enhance the axial resolution of various super-resolution techniques. For instance, iso-STED employs two opposing objectives and an advanced interference scheme for the collected fluorescence to enhance the axial resolution of STED microscopy (87, 96) (**Figure 2*d***). Similarly, interferometric PALM (95) and 4Pi single-molecule switching (109) use interferometric superposition of collected fluorescence to improve axial resolution in SMLM.

The drawback of these methods is that they require a full-fledged interferometer with a wavefront stability of a few nanometers, which is technically challenging. This complexity has limited the broader adoption of these methods in biophysics and the life sciences. An alternative to interferometric methods involves using near-field effects to achieve nanometer axial resolution. The

most straightforward approach utilizes the exponentially decaying intensity of the evanescent field generated above a coverslip when illuminated from the glass side with a plane wave at an incidence angle above the total internal reflection (TIR) angle. This technique, commonly used in TIR fluorescence (TIRF) microscopy, targets structures close to the glass–sample interface. By varying the incidence angle of the TIR excitation and recording corresponding fluorescence images, one can determine the distance of a fluorescent emitter from the surface. This principle, known as variable-angle TIRF (VA-TIRF) microscopy (**Figure 3*b***), has also been applied in SMLM to achieve nanometer-precise axial localization of single molecules (23). However, maintaining fluorophore stability during image series acquisition is challenging. Therefore, we focus on near-field-based methods for axial single-molecule localization that operate instantly with a single image recording.

5.1. Supercritical Angle Fluorescence

The first family of near-field methods for axial localization that we discuss relies on the tunneling of near-field virtual photons from a fluorescent molecule into propagating photon modes in an optically denser medium, typically transitioning from an aqueous solution onto the glass coverslip. This process results in supercritical angle fluorescence (SAF) (**Figure 3*a***), where emission occurs at solid angles above the critical TIR angle between the glass and the sample medium. Fluorescent molecules situated far from the glass surface (about half a wavelength) cannot emit into this angular region, but as an emitter approaches the glass surface, the SAF emission increases, reaching approximately 30% of the total emission for a molecule directly on the glass. By measuring the ratio between the SAF emission intensity and the undercritical angle fluorescence (UAF) emission intensity, one can determine the absolute distance of an emitter from the surface. This method was pioneered by Ruckstuhl and colleagues (114) and further developed by the Lèvêque-Fort group (5) (direct optical nanoscopy with axially localized detection) and the Ries group (20) (supercritical angle localization microscopy) for 3D SMLM with nanometer axial localization accuracy. An extensive description and comparison of SAF microscopy realizations for SMLM is presented in Reference 121.

One challenge of SAF, besides requiring sophisticated measurement setups, is its reliance on relative intensity measurements, which require careful calibration and are susceptible to any effect that modifies the SAF-to-UAF intensity ratio. Slight refractive index modulations in a sample can affect the final axial localization result, as they can alter the SAF-to-UAF intensity ratio of an emitter. A potentially more robust method that utilizes near-field coupling of a fluorescent emitter to surface plasmons or excitons in planar layers is discussed in Section 5.2.

5.2. Metal- and Graphene-Induced Energy Transfer

When a fluorescing molecule is near a metallic nanostructure, such as a metallic nanoparticle or metal layer, its electromagnetic near-field components start to couple to the free electrons in the metal. This interaction allows the molecule to transfer its excited state energy to electron oscillations in the metal, known as plasmons. The efficiency of this energy transfer is highly dependent on the distance between the fluorescent molecule and the metal, forming the basis for MIET imaging (16). In MIET, a conventional microscopy coverslip is coated with a thin metal layer (typically a 20-nm gold film), which induces a predictable distance-dependent fluorescence lifetime modulation in nearby molecules (**Figure 4**). By measuring the fluorescence lifetime of a molecule and applying an appropriate physical model (11), one can convert this lifetime into a precise distance measurement from the surface, achieving nanometer accuracy.

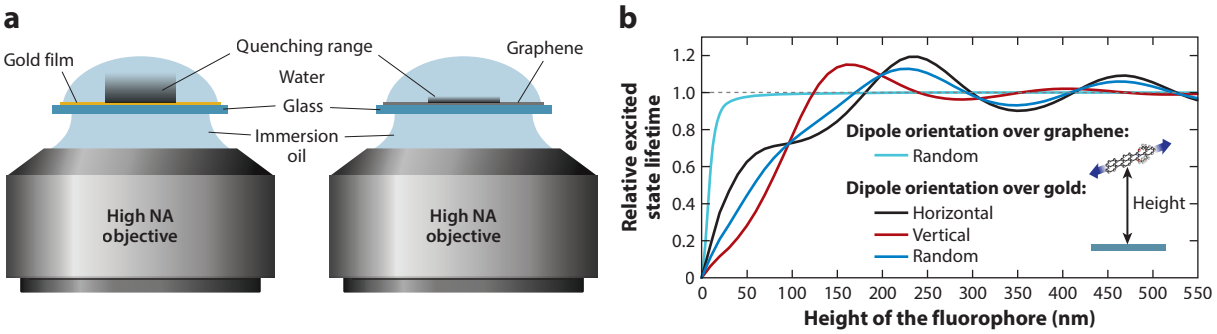

Figure 4

MIET and GIET imaging measure the nanoscale distance between fluorescent molecules and a metal and a graphene surface, respectively. In MIET, energy transfer occurs between the excited fluorophores and the free electrons within a nearby metal layer, leading to strongly distance-dependent fluorescence quenching and thus fluorescence lifetime and intensity modulation. GIET operates similarly, but the energy transfer happens between the fluorophores and excitons in a graphene layer. (*a*) Both techniques allow for precise measurements of distances down to the nanometer scale, making them valuable for studying membrane dynamics, protein interactions, and cellular architecture. However, the dynamic range (the distance range over which the lifetime-versus-distance curve is monotonous) of MIET is approximately eight times larger (up to approximately 250 nm) than the dynamic range for GIET (up to approximately 30 nm). In contrast, GIET allows for an Ångström axial resolution, which is particular useful for 3D SMLM at the molecular level. (*b*) Representative fluorescence lifetime-versus-distance calibration curve for MIET with a 20-nm gold film on glass for fluorescence at 670 nm. The three curves refer to different orientations of a fluorophore's emission dipole with respect to the surface. For samples where the fluorophores are not free to rotate, this orientation has to be measured independently, for example, by defocused imaging (53). Abbreviations: GIET, graphene-induced energy transfer; MIET, metal-induced energy transfer; NA, numerical aperture; SMLM, single-molecule localization microscopy.

MIET imaging is similar to Förster resonance energy transfer (FRET) and SAF imaging. All three methods involve the near-field coupling of an emitting molecule to an acceptor in a distance-dependent manner. In FRET, the acceptor is another molecule with an absorption spectrum that overlaps the emission spectrum of the fluorescing molecule (the so-called donor molecule). In SAF, the acceptor is the bulk glass of the coverslip. In MIET, the acceptor is the free electron gas in the metal layer. Whereas FRET requires knowledge of the three relative angles that describe the orientation of the donor and acceptor molecules (but see Reference 34 about FRET-SMLM), which cannot be measured in totality by independent measurements, MIET and SAF require only the two angles that describe the emitter's orientation relative to the surface, which can be independently measured.

Simultaneous measurement of orientation and 3D position using MIET and polarization-resolved scan imaging was demonstrated by Karedla et al. (53), achieving isotropic nanometer accuracy. This method was further extended by Thiele et al. (104) to resolve the 3D structure of microtubules using FL-SMLM combined with MIET. MIET–FL-SMLM thus shows great promise for achieving isotropic nanometric resolution. Like other near-field methods such as VA-TIRF or SAF, MIET is limited by the spatial extent of the near field, typically approximately 200 nm, but within this range, it can deliver axial resolution of approximately 1 to 2 nm for 10,000 photons.

To improve axial resolution even further, an alternative quenching mechanism using graphene has been proposed. As first pointed out by Moerland & Hoogenboom (65), graphene can induce strong distance-dependent modulation of fluorescence lifetime over a shorter range (approximately 25 nm). This interaction, more akin to FRET, is termed graphene-induced energy transfer (GIET) or graphene energy transfer (GET). Due to its smaller interaction range, GIET offers

increased spatial resolution, as demonstrated by Ghosh et al. (29) and Kamińska et al. (52). GIET imaging has achieved exceptional axial resolution for measuring the thickness of single lipid bilayers both in vitro (14) and in vivo (76) with a resolution of approximately 5 Å. The excellent axial resolution of GIET makes it ideal for molecular level 3D SMLM, as recently demonstrated by combining DNA-PAINT, GIET, and MINFLUX (119). Comprehensive protocols for MIET and GIET experiments have been published (28). Moreover, the Tinnefeld group (30) has shown that using multiple graphene layers can slightly extend the dynamic range of GIET imaging.

6. CRYO-FLUORESCENCE SINGLE-MOLECULE LOCALIZATION MICROSCOPY

As discussed in Section 1, the primary limitation to achieving higher resolution in conventional SMLM techniques like PALM and dSTORM stems from the finite number of emission cycles of single fluorescent molecules before they photobleach. The main goal of PAINT is to overcome this limitation by continuously replenishing the fluorescent label at a given target site. An alternative approach, pursued from the beginning, involves the use of cryo-fluorescence microscopy to enhance the photostability of fluorescent molecules. Cooling fluorescent molecules down to liquid nitrogen or liquid helium temperatures can increase their photostability by several orders of magnitude (**Figure 3*d***), allowing for single-molecule localization accuracy down to 1 Å (56).

The significant challenge here is that this dramatically increased photostability comes at the cost of suppressed photoswitching, which is crucial for SMLM. Whereas little or no blinking is observed at liquid nitrogen temperatures (44), this appears to improve at liquid helium temperatures. Using the residual spontaneous blinking of fluorescent molecules at such temperatures, Sandoghdar and colleagues (113) demonstrated single-molecule colocalization with nanometer resolution and later resolved the four biotin binding sites on a single streptavidin molecule (112). This was a remarkable achievement, but the main challenge remained the relatively small number of target complexes showing sufficient blinking for successful colocalization measurements. This group reviewed the challenges and potential of cryo-SMLM for resolving molecular structures in a recent paper (62).

Substantial efforts have been invested in finding suitable fluorescent emitters that exhibit sufficient photoswitching even under cryogenic conditions. Pioneering work in this area was done by Dahlberg & Moerner (19), focusing on red fluorescent proteins with suitable photoswitching properties. They reported on the proteins roGFP2 (74) and mApple (83) as promising candidates for cryo-SMLM, although slow and uncontrollable switching kinetics still limit their application. Another interesting candidate for cryo-SMLM is the fluorescent protein rsEGFP2, extensively investigated by the Bourgeois group (60, 77), including elucidation of the molecular switching mechanism.

If the goal is to resolve only two molecules on a given target molecule or complex, an interesting alternative to photoswitching is polarization-modulated excitation combined with polarization-resolved detection. This approach was first attempted by Lew and colleagues (122) using complex radially and azimuthally polarized excitation beams in conjunction with polarized multiview detection. Recently, they showed that it is possible to uniquely determine the orientations of two optically unresolvable molecules and subsequently disentangle their positions, provided that their orientations differ by a minimal angle, as low as 10° (15). The major advantage of this approach is its independence from the photoswitching properties of the fluorescent molecules, making it ideal for cryo-SMLM where the orientations of all emitters are fixed. Considering the vast available photon budget per molecule in cryo-SMLM, this method could revolutionize colocalizing two molecules with Ångström resolution, offering a highly promising alternative to similar attempts using single-molecule FRET (1).

7. CALIBRATION AND DATA ANALYSIS

An important issue of molecular level SMLM is the precise calibration and performance validation of an SMLM system using well-defined and easy-to-handle rulers. Additionally, the optimal evaluation of recorded data is crucial for achieving maximum accuracy and precise single-molecule localizations. This is the focus of this final section.

7.1. Calibration and Validation Tools

To ensure the reliability and accuracy of SMLM measurements, the use of calibration standards is essential. These standards typically include DNA origami structures, protein-based nanorulers, and virus-based nanorulers. These structures are designed with precise distances between fluorophores, allowing researchers to verify the resolution and accuracy of their SMLM systems.

DNA origami is a popular tool for calibration due to its customizable and precise structural features. It allows for the placement of fluorophores at known distances, providing a robust standard for verifying SMLM resolution and accuracy (88, 100). DNA origami can be designed in both 2D and 3D configurations, making it versatile for various calibration needs (57, 84). Recently, DNA origamis were used for calibrating and validating 3D GIET/GET imaging (51). One challenge of DNA origami rulers is the complexity of their design and correct prediction of the structure of the single DNA strands used for their synthesis, and another challenge is that their actual structure can also be very dependent on environmental factors such as the salt concentrations of the buffers that are required for their stability.

As an alternative, protein-based nanorulers can be used. They are created using proteins with defined binding sites for fluorophores. One example is the use of microtubules, but the most popular among them are nuclear pore complexes, which represent natural nanorulers due to their known and consistent structural features (85, 102). An alternative, genetic code expansion was used to incorporate single fluorescent molecules with a spacing as low as 6 nm into the homotrimeric protein complex proliferating cell nuclear antigen to generate a molecular level SMLM ruler (40).

Finally, virus-based nanorulers seem to be an attractive alternative to DNA origamis and protein structures. Viruses, due to their uniform size and stable structure, could serve as excellent nanorulers for SMLM calibration. The T4 phage has been recently reported as a highly reproducible and perfectly orientable structure for SMLM 3D calibration (26).

7.2. Data Evaluation and Analysis

Evaluating recorded data in SMLM requires meticulous attention to extract precise single-molecule localizations. Advanced algorithms and software tools are employed to process the data, correct for drift, and minimize noise, thereby enhancing the final resolution. The most popular SMLM algorithms, such as ThunderSTORM (71) and rapidSTORM (116), provide robust frameworks for analyzing SMLM data. These tools offer various fitting algorithms, drift correction methods, and visualization options. Achieving high accuracy in SMLM necessitates correcting for sample drift during image acquisition. The new MATLAB toolbox SMITE should also be mentioned (89); it integrates a wealth of SMLM and particle-tracking analysis tools. Additionally, the SMLM and single-molecule tracking package Track-N-Trace (99) offers single-molecule fluorescence lifetime fitting for analyzing FL-SMLM data.

For molecular level SMLM, the requirements for optimal localization algorithms, drift correction, and noise reduction become even more stringent. In recent years, two approaches in SMLM data analysis have gained increasing attention: rigorous Bayesian inference treatment of data, based on a comprehensive model of the entire SMLM experiment, and machine learning approaches using advanced neural networks.

In PAINT imaging, a significant challenge is correctly attributing repeated single-molecule localizations to the correct target position, especially when the distance between targets becomes close to or smaller than the localization accuracy of one binding event. As discussed above, sequential imaging as realized by RESI is one solution. Additionally, sophisticated data analysis approaches can assist in this direction. A Bayesian approach to correctly grouping single-molecule events in SMLM was discussed by Fazel et al. (25). Similarly, Ries and colleagues (117) have used rigorous maximum-likelihood estimators for SMLM. Particle fusion (110) and particle averaging (42) were used to generate high-resolution structures of interest by compounding SMLM data from many individual structures. The Pressé group (24), in collaboration with several collaborators around the world, has published a comprehensive review on Bayesian analysis of SMLM, which is expected to become the gold standard for such methods in the future.

An alternative to full probabilistic models are deep learning approaches in SMLM data analysis, which have seen significant advances over the past few years. Pioneering work in this area has been done by Moerner and colleagues (48, 64) and Shechtman and colleagues (82). For an excellent review on deep learning approaches in super-resolution microscopy, see Reference 63, and a recent tutorial can be found in Reference 58.

8. DISCUSSION AND OUTLOOK

In this review, we have aimed to present a comprehensive overview of the various methods and approaches to molecular level super-resolution microscopy, with a particular focus on SMLM. Due to length constraints, we have inevitably left out many intriguing ideas and emerging techniques. For instance, we did not cover the innovative use of temporally modulated excitation patterns for converting temporally imprinted intensity modulation into single-molecule localizations (45–47) or other promising concepts such as tip-enhanced single-molecule luminescence for Ångström-resolution imaging (118).

Based on the information and literature discussed in this review, the most promising contenders for achieving molecular level super-resolution microscopy appear to be RESI, PAINT-MINFLUX, and polarization cryo-fluorescence microscopy (for two-molecule colocalization), potentially in combination with axial localization approaches such as SAF or MIET. In particular, RESI seems to be the most straightforward method to implement and holds the potential to revolutionize the application of fluorescence microscopy for elucidating structural details in single proteins and biomolecular complexes. This advancement will add specificity to the superb electron density maps provided by electron microscopy.

DISCLOSURE STATEMENT

The authors are not aware of any affiliations, memberships, funding, or financial holdings that might be perceived as affecting the objectivity of this review.

ACKNOWLEDGMENTS

N.R. and J.E. acknowledge financial support from the Bundesministerium für Bildung und Forschung of Germany via project NG-FLIM (13N15327 and 13N15328). J.I.G. acknowledges financial support from the European Union's Horizon 2021 research and innovation program under the Marie Skłodowska-Curie grant agreement 101062508 (project name: SOADOPP). J.E. and J.I.G. acknowledge financial support by the Deutsche Forschungsgemeinschaft through Germany's Excellence Strategy EXC 2067/1-390729940. J.E., O.N., and N.R. thank the European Research Council for financial support via project "smMIET" (grant agreement 884488) under the European Union's Horizon 2020 research and innovation program.

LITERATURE CITED

1. Agam G, Gebhardt C, Popara M, Mächtel R, Folz J, et al. 2023. Reliability and accuracy of single-molecule FRET studies for characterization of structural dynamics and distances in proteins. *Nat. Methods* 20(4):523–35
2. Alvelid J, Testa I. 2019. Fluorescence microscopy at the molecular scale. *Curr. Opin. Biomed. Eng.* 12:34–42
3. Balzarotti F, Eilers Y, Gwosch KC, Gynnå AH, Westphal V, et al. 2017. Nanometer resolution imaging and tracking of fluorescent molecules with minimal photon fluxes. *Science* 355(6325):606–12
4. Betzig E, Patterson GH, Sougrat R, Lindwasser OW, Olenych S, et al. 2006. Imaging intracellular fluorescent proteins at nanometer resolution. *Science* 313(5793):1642–45
5. Bourg N, Mayet C, Dupuis G, Barroca T, Bon P, et al. 2015. Direct optical nanoscopy with axially localized detection. *Nat. Photon.* 9(9):587–93
6. Bowman AJ, Klopfer BB, Juffmann T, Kasevich MA. 2019. Electro-optic imaging enables efficient wide-field fluorescence lifetime microscopy. *Nat. Commun.* 10(1):4561
7. Bucci A, Tortarolo G, Held MO, Bega L, Perego E, et al. 2024. 4D single-particle tracking with asynchronous read-out single-photon avalanche diode array detector. *Nat. Commun.* 15:6188
8. Buttafava M, Villa F, Castello M, Tortarolo G, Conca E, et al. 2020. SPAD-based asynchronous-readout array detectors for image-scanning microscopy. *Optica* 7(7):755–65
9. Carsten A, Rudolph M, Weihs T, Schmidt R, Jansen I, et al. 2022. MINFLUX imaging of a bacterial molecular machine at nanometer resolution. *Methods Appl. Fluoresc.* 11(1):015004
10. Castello M, Tortarolo G, Buttafava M, Deguchi T, Villa F, et al. 2019. A robust and versatile platform for image scanning microscopy enabling super-resolution FLIM. *Nat. Methods* 16(2):175–78
11. Chance R, Prock A, Silbey R. 1978. Molecular fluorescence and energy transfer near interfaces. *Adv. Chem. Phys.* 37:1–65
12. Chang TJB, Hsu JCC, Yang TT. 2023. Single-molecule localization microscopy reveals the ultrastructural constitution of distal appendages in expanded mammalian centrioles. *Nat. Commun.* 14(1):1688
13. Chen F, Tillberg PW, Boyden ES. 2015. Expansion microscopy. *Science* 347(6221):543–48
14. Chen T, Ghosh A, Enderlein J. 2023. Cholesterol-induced nanoscale variations in the thickness of phospholipid membranes. *Nano Lett.* 23(6):2421–26
15. Chen Y, Qiu Y, Lew MD. 2024. Resolving the orientations of and separation between an overlapping pair of dipole emitters. arXiv:2406.04469 [physics.optics]
16. Chizhik AI, Rother J, Gregor I, Janshoff A, Enderlein J. 2014. Metal-induced energy transfer for live cell nanoscopy. *Nat. Photon.* 8(2):124–27
17. Chozinski TJ, Halpern AR, Okawa H, Kim HJ, Tremel GJ, et al. 2016. Expansion microscopy with conventional antibodies and fluorescent proteins. *Nat. Methods* 13(6):485–88
18. Cnossen J, Hinsdale T, Thorsen RO, Siemons M, Schueder F, et al. 2020. Localization microscopy at doubled precision with patterned illumination. *Nat. Methods* 17(1):59–63
19. Dahlberg PD, Moerner WE. 2021. Cryogenic super-resolution fluorescence and electron microscopy correlated at the nanoscale. *Annu. Rev. Phys. Chem.* 72:253–78
20. Dasgupta A, Deschamps J, Matti U, Hübner U, Becker J, et al. 2021. Direct supercritical angle localization microscopy for nanometer 3D superresolution. *Nat. Commun.* 12(1):1180
21. Deguchi T, Ries J. 2024. Simple and robust 3D MINFLUX excitation with a variable phase plate. *Light Sci. Appl.* 13(1):134
22. Egner A, Jakobs S, Hell SW. 2002. Fast 100-nm resolution three-dimensional microscope reveals structural plasticity of mitochondria in live yeast. *PNAS* 99(6):3370–75
23. Fan D, Cnossen J, Hung ST, Kromm D, Dekker NH, et al. 2023. Three-dimensional localization microscopy with increased axial precision through TIRF angle modulation. *Opt. Commun.* 542:129548
24. Fazel M, Grussmayer KS, Ferdman B, Radenovic A, Shechtman Y, et al. 2024. Fluorescence microscopy: a statistics-optics perspective. *Rev. Mod. Phys.* 96(2):025003
25. Fazel M, Wester MJ, Schodt DJ, Cruz SR, Strauss S, et al. 2022. High-precision estimation of emitter positions using Bayesian grouping of localizations. *Nat. Commun.* 13(1):7152

26. Gallea JI, Nevskyi O, Kaźmierczak Z, Chen T, Miernikiewicz P, et al. 2024. Super-resolution going viral: T4 virus particles as perfect nature-designed 3D-bio-NanoRulers. bioRxiv 2024.04.04.588072. **https://doi.org/10.1101/2024.04.04.588072**
27. Gambarotto D, Zwettler FU, Le Guennec M, Schmidt-Cernohorska M, Fortun D, et al. 2019. Imaging cellular ultrastructures using expansion microscopy (U-ExM). *Nat. Methods* 16(1):71–74
28. Ghosh A, Chizhik AI, Karedla N, Enderlein J. 2021. Graphene- and metal-induced energy transfer for single-molecule imaging and live-cell nanoscopy with (sub)-nanometer axial resolution. *Nat. Protoc.* 16(7):3695–715
29. Ghosh A, Sharma A, Chizhik AI, Isbaner S, Ruhlandt D, et al. 2019. Graphene-based metal-induced energy transfer for sub-nanometre optical localization. *Nat. Photon.* 13:860–65
30. Gronkiewicz K, Richter L, Knechtel F, Pyrcz P, Leidinger P, et al. 2024. Expanding the range of graphene energy transfer with multilayer graphene. *Nanoscale* 16(28):13464–70
31. Gustafsson MG. 1999. Extended resolution fluorescence microscopy. *Curr. Opin. Struct. Biol.* 9(5):627–28
32. Gustafsson MG, Agard DA, Sedat JW. 1999. I^5M: 3D widefield light microscopy with better than 100 nm axial resolution. *J. Microsc.* 195(Part 1):10–16
33. Gwosch KC, Pape JK, Balzarotti F, Hoess P, Ellenberg J, et al. 2020. MINFLUX nanoscopy delivers 3D multicolor nanometer resolution in cells. *Nat. Methods* 17:217–24
34. Ha T, Fei J, Schmid S, Lee NK, Gonzalez RL, et al. 2024. Fluorescence resonance energy transfer at the single-molecule level. *Nat. Rev. Methods Primers* 4(1):1–18
35. Heilemann M, van de Linde S, Mukherjee A, Sauer M. 2009. Super-resolution imaging with small organic fluorophores. *Angew. Chem. Int. Ed. Engl.* 48(37):6903–8
36. Heintzmann R, Huser T. 2017. Super-resolution structured illumination microscopy. *Chem. Rev.* 117(23):13890–908
37. Hell S, Stelzer EHK. 1992. Fundamental improvement of resolution with a 4Pi-confocal fluorescence microscope using two-photon excitation. *Opt. Commun.* 93(5):277–82
38. Hell SW, Wichmann J. 1994. Breaking the diffraction resolution limit by stimulated emission: stimulated-emission-depletion fluorescence microscopy. *Opt Lett.* 19(11):780–82
39. Helmerich DA, Beliu G, Taban D, Meub M, Streit M, et al. 2022. Photoswitching fingerprint analysis bypasses the 10-nm resolution barrier. *Nat. Methods* 19(88):986–94
40. Helmerich DA, Budiarta M, Taban D, Doose S, Beliu G, Sauer M. 2024. PCNA as protein-based nanoruler for sub-10 nm fluorescence imaging. *Adv. Mater.* 36(7):2310104
41. Hess ST, Girirajan TPK, Mason MD. 2006. Ultra-high resolution imaging by fluorescence photoactivation localization microscopy. *Biophys. J.* 91(11):4258–72
42. Heydarian H, Joosten M, Przybylski A, Schueder F, Jungmann R, et al. 2021. 3D particle averaging and detection of macromolecular symmetry in localization microscopy. *Nat. Commun.* 12(11):2847
43. Huang B, Wang W, Bates M, Zhuang X. 2008. Three-dimensional super-resolution imaging by stochastic optical reconstruction microscopy. *Science* 319(5864):810–13
44. Hulleman CN, Li W, Gregor I, Rieger B, Enderlein J. 2018. Photon yield enhancement of red fluorophores at cryogenic temperatures. *ChemPhysChem* 19(14):1774–80
45. Illand A, Jouchet P, Fort E, Lévêque-Fort S. 2024. Flexible implementation of modulated localisation microscopy based on DMD. *J. Microsc.* 295(1):21–32
46. Jouchet P, Cabriel C, Bourg N, Bardou M, Poüs C, et al. 2021. Nanometric axial localization of single fluorescent molecules with modulated excitation. *Nat. Photon.* 15:297–304
47. Jouchet P, Poüs C, Fort E, Lévêque-Fort S. 2022. Time-modulated excitation for enhanced single-molecule localization microscopy. *Philos. Trans. R. Soc. A* 380(2220):20200299
48. Jouchet P, Roy AR, Moerner WE. 2023. Combining deep learning approaches and point spread function engineering for simultaneous 3D position and 3D orientation measurements of fluorescent single molecules. *Opt. Commun.* 542:129589
49. Juette MF, Gould TJ, Lessard MD, Mlodzianoski MJ, Nagpure BS, et al. 2008. Three-dimensional sub–100 nm resolution fluorescence microscopy of thick samples. *Nat. Methods* 5(6):527–29
50. Jungmann R, Steinhauer C, Scheible M, Kuzyk A, Tinnefeld P, Simmel FC. 2010. Single-molecule kinetics and super-resolution microscopy by fluorescence imaging of transient binding on DNA origami. *Nano Lett.* 10(11):4756–61

51. Kaminska I, Bohlen J, Rocchetti S, Selbach F, Acuna GP, Tinnefeld P. 2019. Distance dependence of single-molecule energy transfer to graphene measured with DNA origami nanopositioners. *Nano Lett.* 19(7):4257–62
52. Kamińska I, Bohlen J, Yaadav R, Schüler P, Raab M, et al. 2021. Graphene energy transfer for single-molecule biophysics, biosensing, and super-resolution microscopy. *Adv. Mater.* 33(24):2101099
53. Karedla N, Chizhik AM, Stein SC, Ruhlandt D, Gregor I, et al. 2018. Three-dimensional single-molecule localization with nanometer accuracy using metal-induced energy transfer (MIET) imaging. *J. Chem. Phys.* 148(20):204201
54. Koho SV, Slenders E, Tortarolo G, Castello M, Buttafava M, et al. 2020. Two-photon image-scanning microscopy with SPAD array and blind image reconstruction. *Biomed. Opt. Express* 11(6):2905–24
55. Lee H-LD, Sahl SJ, Lew MD, Moerner WE. 2012. The double-helix microscope super-resolves extended biological structures by localizing single blinking molecules in three dimensions with nanoscale precision. *Appl. Phys. Lett.* 100(15):153701
56. Li W, Stein SC, Gregor I, Enderlein J. 2015. Ultra-stable and versatile widefield cryo-fluorescence microscope for single-molecule localization with sub-nanometer accuracy. *Opt. Express* 23(3):3770
57. Lin R, Clowsley AH, Lutz T, Baddeley D, Soeller C. 2020. 3D super-resolution microscopy performance and quantitative analysis assessment using DNA-PAINT and DNA origami test samples. *Methods* 174:56–71
58. Liu J, Li Y, Chen T, Zhang F, Xu F. 2024. Machine learning for single-molecule localization microscopy: from data analysis to quantification. *Anal. Chem.* 96(28):11103–14
59. Liu S, Hoess P, Ries J. 2022. Super-resolution microscopy for structural cell biology. *Annu. Rev. Biophys.* 51:301–26
60. Mantovanelli AMR, Glushonkov O, Adam V, Wulffelé J, Thédié D, et al. 2023. Photophysical studies at cryogenic temperature reveal a novel photoswitching mechanism of rsEGFP2. *J. Am. Chem. Soc.* 145(27):14636–46
61. Masullo LA, Steiner F, Zähringer J, Lopez LF, Bohlen J, et al. 2020. Pulsed interleaved MINFLUX. *Nano Lett.* 21(1):840–46
62. Mazal H, Wieser FF, Sandoghdar V. 2023. Insights into protein structure using cryogenic light microscopy. *Biochem. Soc. Trans.* 51(6):2041–59
63. Möckl L, Roy AR, Moerner WE. 2020. Deep learning in single-molecule microscopy: fundamentals, caveats, and recent developments. *Biomed. Opt. Express* 11(3):1633–61
64. Möckl L, Roy AR, Petrov PN, Moerner WE. 2020. Accurate and rapid background estimation in single-molecule localization microscopy using the deep neural network bgnet. *PNAS* 117(1):60–67
65. Moerland RJ, Hoogenboom JP. 2016. Subnanometer-accuracy optical distance ruler based on fluorescence quenching by transparent conductors. *Optica* 3(2):112–17
66. Mortensen KI, Churchman LS, Spudich JA, Flyvbjerg H. 2010. Optimized localization analysis for single-molecule tracking and super-resolution microscopy. *Nat. Methods* 7(5):377–81
67. Müller CB, Enderlein J. 2010. Image scanning microscopy. *Phys. Rev. Lett.* 104(19):198101
68. Oleksiievets N, Mathew C, Thiele JC, Gallea JI, Nevskyi O, et al. 2022. Single-molecule fluorescence lifetime imaging using wide-field and confocal-laser scanning microscopy: a comparative analysis. *Nano Lett.* 22(15):6454–61
69. Oleksiievets N, Thiele JC, Weber A, Gregor I, Nevskyi O, et al. 2020. Wide-field fluorescence lifetime imaging of single molecules. *J. Phys. Chem. A* 124(17):3494–500
70. Ostersehlt LM, Jans DC, Wittek A, Keller-Findeisen J, Inamdar K, et al. 2022. DNA-PAINT MINFLUX nanoscopy. *Nat. Methods* 19:1072–75
71. Ovesnỳ M, Křížek P, Borkovec J, Švindrych Z, Hagen GM. 2014. ThunderSTORM: a comprehensive ImageJ plug-in for PALM and STORM data analysis and super-resolution imaging. *Bioinformatics* 30(16):2389–90
72. Pape JK, Stephan T, Balzarotti F, Büchner R, Lange F, et al. 2020. Multicolor 3D MINFLUX nanoscopy of mitochondrial MICOS proteins. *PNAS* 117(34):20607–14
73. Pavani SRP, Thompson MA, Biteen JS, Lord SJ, Liu N, et al. 2009. Three-dimensional, single-molecule fluorescence imaging beyond the diffraction limit by using a double-helix point spread function. *PNAS* 106(9):2995–99

74. Perez D, Dahlberg PD, Wang J, Sartor AM, Borden JS, et al. 2022. Identification and demonstration of roGFP2 as an environmental sensor for cryogenic correlative light and electron microscopy. *J. Struct. Biol.* 214(3):107881
75. Radmacher N, Nevskyi O, Gallea JI, Thiele JC, Gregor I, et al. 2024. Doubling the resolution of fluorescence-lifetime single-molecule localization microscopy with image scanning microscopy. 18:1059–66
76. Raja SO, Chizhik AI, Schmidt CF, Enderlein J, Ghosh A. 2021. Mapping activity-dependent quasi-stationary states of mitochondrial membranes with graphene-induced energy transfer imaging. *Nano Lett.* 21(19):8244–49
77. Rane L, Wulffele J, Bourgeois D, Glushonkov O, Mantovanelli AMR, et al. 2023. Light-induced forward and reverse intersystem crossing in green fluorescent proteins at cryogenic temperatures. *J. Phys. Chem. B* 127(22):5046–54
78. Reinhardt SCM, Masullo LA, Baudrexel I, Steen PR, Kowalewski R, et al. 2023. Ångström-resolution fluorescence microscopy. *Nature* 617(79627962):711–16
79. Reymond L, Huser T, Ruprecht V, Wieser S. 2020. Modulation-enhanced localization microscopy. *J. Phys. Photon.* 2(4):041001
80. Reymond L, Reymond L, Ziegler J, Knapp C, Wang FC, et al. 2019. SIMPLE: structured illumination based point localization estimator with enhanced precision. *Opt. Express* 27(17):24578–90
81. Rust MJ, Bates M, Zhuang X. 2006. Sub-diffraction-limit imaging by stochastic optical reconstruction microscopy (STORM). *Nat Methods*. 3(10):793–95
82. Saguy A, Alalouf O, Opatovski N, Jang S, Heilemann M, Shechtman Y. 2023. DBlink: dynamic localization microscopy in super spatiotemporal resolution via deep learning. *Nat. Methods* 20(12):1939–48
83. Sartor AM, Dahlberg PD, Perez D, Moerner WE. 2023. Characterization of mApple as a red fluorescent protein for cryogenic single-molecule imaging with turn-off and turn-on active control mechanisms. *J. Phys. Chem. B* 127(12):2690–700
84. Scheckenbach M, Bauer J, Zähringer J, Selbach F, Tinnefeld P. 2020. DNA origami nanorulers and emerging reference structures. *APL Mater.* 8(11):110902
85. Schlichthaerle T, Strauss MT, Schueder F, Auer A, Nijmeijer B, et al. 2019. Direct visualization of single nuclear pore complex proteins using genetically-encoded probes for DNA-PAINT. *Angew. Chem. Int. Ed. Engl.* 58(37):13004–8
86. Schmidt R, Weihs T, Wurm CA, Jansen I, Rehman J, et al. 2021. MINFLUX nanometer-scale 3D imaging and microsecond-range tracking on a common fluorescence microscope. *Nat. Commun.* 12(11):1478
87. Schmidt R, Wurm CA, Jakobs S, Engelhardt J, Egner A, Hell SW. 2008. Spherical nanosized focal spot unravels the interior of cells. *Nat. Methods* 5(6):539–44
88. Schmied JJ, Raab M, Forthmann C, Pibiri E, Wünsch B, et al. 2014. DNA origami–based standards for quantitative fluorescence microscopy. *Nat. Protoc.* 9(6):1367–91
89. Schodt DJ, Wester MJ, Fazel M, Khan S, Mazloom-Farsibaf H, et al. 2023. Smite: single molecule imaging toolbox extraordinaire (MATLAB). *J. Open Source Softw.* 8(90):5563
90. Schueder F, Stein J, Stehr F, Auer A, Sperl B, et al. 2019. An order of magnitude faster DNA-PAINT imaging by optimized sequence design and buffer conditions. *Nat. Methods* 16:1101–4
91. Shaib AH, Chouaib AA, Chowdhury R, Mihaylov D, Zhang C, et al. 2023. Visualizing proteins by expansion microscopy. bioRxiv 2022.08.03.502284. **https://doi.org/10.1101/2022.08.03.502284**
92. Sharonov A, Hochstrasser RM. 2006. Wide-field subdiffraction imaging by accumulated binding of diffusing probes. *PNAS* 103(50):18911–16
93. Shechtman Y, Weiss LE, Backer AS, Sahl SJ, Moerner WE. 2015. Precise three-dimensional scan-free multiple-particle tracking over large axial ranges with tetrapod point spread functions. *Nano Lett.* 15(6):4194–99
94. Sheppard CJ. 1988. Super-resolution in confocal imaging. *Optik* 80(2):53–54
95. Shtengel G, Galbraith JA, Galbraith CG, Lippincott-Schwartz J, Gillette JM, et al. 2009. Interferometric fluorescent super-resolution microscopy resolves 3D cellular ultrastructure. *PNAS* 106(9):3125–30

96. Siegmund R, Werner F, Jakobs S, Geisler C, Egner A. 2021. isoSTED microscopy with water-immersion lenses and background reduction. *Biophys. J.* 120(16):3303–14
97. Slenders E, Perego E, Buttafava M, Tortarolo G, Conca E, et al. 2021. Cooled SPAD array detector for low light-dose fluorescence laser scanning microscopy. *Biophys. Rep.* 1(2):100025
98. Slenders E, Vicidomini G. 2023. ISM-FLUX: MINFLUX with an array detector. *Phys. Rev. Res.* 5(2):023033
99. Stein SC, Thiart J. 2016. TrackNTrace: a simple and extendable open-source framework for developing single-molecule localization and tracking algorithms. *Sci. Rep.* 6(1):37947
100. Steinhauer C, Jungmann R, Sobey TL, Simmel FC, Tinnefeld P. 2009. DNA origami as a nanoscopic ruler for super-resolution microscopy. *Angew. Chem. Int. Ed. Engl.* 48(47):8870–73
101. Strauss S, Jungmann R. 2020. Up to 100-fold speed-up and multiplexing in optimized DNA-PAINT. *Nat. Methods* 17(8):789–91
102. Thevathasan JV, Kahnwald M, Cieśliński K, Hoess P, Peneti SK, et al. 2019. Nuclear pores as versatile reference standards for quantitative superresolution microscopy. *Nat. Methods* 16(10):1045–53
103. Thiele JC, Helmerich DA, Oleksiievets N, Tsukanov R, Butkevich E, et al. 2020. Confocal fluorescence-lifetime single-molecule localization microscopy. *ACS Nano* 14(10):14190–200
104. Thiele JC, Jungblut M, Helmerich DA, Tsukanov R, Chizhik A, et al. 2021. Isotropic three-dimensional dual-color super-resolution microscopy with metal-induced energy transfer. *Sci. Adv.* 8:14190–200
105. Thiele JC, Nevskyi O, Helmerich DA, Sauer M, Enderlein J. 2021. Advanced data analysis for fluorescence-lifetime single-molecule localization microscopy. *Front. Bioinform.* 1:740281
106. Tillberg PW, Chen F, Piatkevich KD, Zhao Y, Yu CCJ, et al. 2016. Protein-retention expansion microscopy of cells and tissues labeled using standard fluorescent proteins and antibodies. *Nat. Biotechnol.* 34(9):987–92
107. van Velde P, Rieger B, Hindsdale T, Cnossen J, Fan D, et al. 2023. ZIMFLUX: single molecule localization microscopy with patterned illumination in 3D. *Opt. Express* 31(25):42701–22
108. von Diezmann A, Shechtman Y, Moerner WE. 2017. Three-dimensional localization of single molecules for super-resolution imaging and single-particle tracking. *Chem. Rev.* 117(11):7244–75
109. Wang J, Allgeyer ES, Sirinakis G, Zhang Y, Hu K, et al. 2020. Implementation of a 4Pi-SMS super-resolution microscope. *Nat. Protoc.* 16:677–727
110. Wang W, Jakobi A, Wu YL, Ries J, Stallinga S, Rieger B. 2023. Particle fusion of super-resolution data reveals the unit structure of Nup96 in nuclear pore complex. *Sci. Rep.* 13(11):13327
111. Wassie AT, Zhao Y, Boyden ES. 2019. Expansion microscopy: principles and uses in biological research. *Nat. Methods* 16(1):33–41
112. Weisenburger S, Boening D, Schomburg B, Giller K, Becker S, et al. 2017. Cryogenic optical localization provides 3D protein structure data with Angstrom resolution. *Nat. Methods* 14(2):141–44
113. Weisenburger S, Jing B, Hänni D, Reymond L, Schuler B, et al. 2014. Cryogenic colocalization microscopy for nanometer-distance measurements. *ChemPhysChem* 15(4):763–70
114. Winterflood CM, Ruckstuhl T, Verdes D, Seeger S. 2010. Nanometer axial resolution by three-dimensional supercritical angle fluorescence microscopy. *Phys. Rev. Lett.* 105(10):108103
115. Wirth JO, Scheiderer L, Engelhardt T, Engelhardt J, Matthias J, Hell SW. 2023. MINFLUX dissects the unimpeded walking of kinesin-1. *Science* 379(6636):1004–10
116. Wolter S, Löschberger A, Holm T, Aufmkolk S, Dabauvalle M-C, et al. 2012. rapidSTORM: accurate, fast open-source software for localization microscopy. *Nat. Methods* 9(11):1040–41
117. Wu YL, Hoess P, Tschanz A, Matti U, Mund M, Ries J. 2023. Maximum-likelihood model fitting for quantitative analysis of SMLM data. *Nat. Methods* 20(1):139–48
118. Yang B, Chen G, Ghafoor A, Zhang Y, Zhang Y, et al. 2020. Sub-nanometre resolution in single-molecule photoluminescence imaging. *Nat. Photon.* 14:693–99
119. Zähringer J, Cole F, Bohlen J, Steiner F, Kamińska I, Tinnefeld P. 2023. Combining pMINFLUX, graphene energy transfer and DNA-PAINT for nanometer precise 3D super-resolution microscopy. *Light Sci. Appl.* 12(11):70
120. Zdańkowski P, Lopez LF, Acuna GP, Stefani FD. 2022. Nanometer resolution imaging and tracking of single fluorophores by sequential structured illumination. *ACS Photon.* 9(12):3777–85

121. Zelger P, Bodner L, Offterdinger M, Velas L, Schütz GJ, Jesacher A. 2021. Three-dimensional single molecule localization close to the coverslip: a comparison of methods exploiting supercritical angle fluorescence. *Biomed. Opt. Express* 12(2):802–22
122. Zhang O, Guo Z, He Y, Wu T, Vahey MD, Lew MD. 2023. Six-dimensional single-molecule imaging with isotropic resolution using a multi-view reflector microscope. *Nat. Photon.* 17(2):179–86
123. Zwettler FU, Reinhard S, Gambarotto D, Bell TDM, Hamel V, et al. 2020. Molecular resolution imaging by post-labeling expansion single-molecule localization microscopy (Ex-SMLM). *Nat. Commun.* 11(11):3388